

Entangled System of Squarks from the Third Generation at the Large Hadron Collider

AseshKrishna Datta¹ and Saurabh Niyogi²

Regional Centre for Accelerator-based Particle Physics (RECAPP)

Harish-Chandra Research Institute

Chhatnag Road, Jhansi, Allahabad, India 211019

Abstract

In the Minimal Supersymmetric extension of the Standard Model (MSSM) squarks from the third generation, i.e., the bottom and the top squarks, have a common set of parameters that determine their masses and couplings. These are in the form of the common soft mass for the left handed squark from the third generation ($m_{\tilde{Q}_{3L}}$), the supersymmetry conserving Higgsino mass parameter μ and $\tan \beta$, the ratio of vacuum expectation values of the two Higgs doublets. This leads to an interesting possibility that the systems involving the bottom and the top squarks might get correlated in a non-trivial way even in an unconstrained setup. In this work, phenomenology of the bottom and the top squarks is studied at the Large Hadron Collider which exploits such a possibility with a particular emphasis on bottom squark decaying to top squark and W boson. Possibility of reconstructing multiple W bosons in the final state is identified to be the key in probing the squark mixing angles. Further entanglement of the electroweak gaugino-higgsino sector is also not impossible in scenarios based on phenomenological MSSM while for highly constrained scenarios like minimal supergravity/constrained MSSM such entanglements are trivially forced upon.

¹asesh@hri.res.in

²sourabh@hri.res.in

1 Introduction

The Large Hadron Collider (LHC), by entering into the data-taking phase, has ushered a new era in high energy physics phenomenology. As of now, each of ATLAS and CMS experiments has collected more than 5.5 fb^{-1} of data. Data analysed so far, either published or preliminary in nature and ranging from 35 pb^{-1} to about 2 fb^{-1} , are yet to point out any clear evidence of physics beyond the Standard Model (SM) of particle physics. Thus, the results presented till date are mostly in terms of setting exclusion limits on the otherwise viable regions of the parameter space of different plausible scenarios beyond the SM. For Supersymmetry (SUSY) as one such viable frameworks to go beyond the SM, the recent LHC analyses [1, 2, 3, 4, 5, 6, 7, 8, 9, 10, 11, 12, 13, 14, 15, 16, 17, 18, 19], have aggressively extended the region already excluded by Tevatron.

While these are definite and quick improvements over what we knew before the LHC data was available, the actual implications of them, at this juncture, should be put in perspective. The single most important thing the LHC experiments (the ATLAS and the CMS in particular, which are in context of the present work) opened up before us is that how powerful and efficient these are to reach out to new regimes in the energy scales. On the other hand, it is appreciated for quite sometime now that a particular SUSY scenario like the minimal Supergravity (mSUGRA) (or, for that matter, the constrained version of the Minimal Supersymmetric Standard Model (the so-called CMSSM)) in which Tevatron carried out most of its analyses and LHC might be sticking to for some more time to come, is at best an extremely special but nonetheless, a useful benchmark for any first study. So, time is just right to move on to explore the chances of how much or what aspects of an (essentially) unconstrained SUSY scenarios could, in principle, be put in the context of experimental observations. Efforts in this direction are already on [20, 21]. In fact, in some of their recent studies, the ATLAS and CMS collaborations had also presented exclusion plots in a framework like the much relaxed phenomenological MSSM [3, 7, 8, 9, 16] and also referred to the so-called *simplified* models [2, 5, 11] following Refs.[22, 23, 24].

Under the circumstances, the SUSY partners of the third generation quarks (the scalar quark or squarks) have got a special standing from a few different but somewhat compelling considerations. For example, it is well known that the squarks from the third generation, *viz.*, the top squark(s) or the ‘stop’ (\tilde{t}) and the bottom squarks(s) or the sbottom (\tilde{b}), may be rather light (compared to their first two generation peers) due to two primary reasons. First, in a high scale scenario where soft SUSY breaking masses are defined at a high scale, the ones for the third generation run down to a much lower value at the weak scale due to the large Yukawa couplings they have. Thus, at the weak scale, the diagonal entries in the scalar mass-squared matrices are generically smaller than those from the first two generations. This is the so-called inverted mass hierarchy [25, 26, 27, 28] where the scalar (SUSY) partners of the massive SM fermions turn out to have smaller soft-masses and vice versa. In addition, as electroweak symmetry breaks, large mixing of the chiral states driven

primarily by the mass of the partner fermions (the top and the bottom quarks) contributes to further lowering of the mass eigenvalues for the third generation sfermions.

Adhering to a somewhat conservative interpretation of the LHC constraints, thus expecting, in general, super-TeV masses for the gluino and the squarks from the first two generations [29], a legitimate search strategy may be to focus on the squarks from the third generation [30, 31]. In any case, irrespective of what lower limits are set by an experiment on the first two generation squark masses, it is always reasonable to expect them to be rather heavy to satisfy different SUSY flavour constraints while allowing for lighter third generation squarks with which the constraints are still much relaxed. Also, recent dedicated studies at ATLAS and CMS on final states involving b -jets [7, 8, 9, 14, 19] in scenarios, where only \tilde{b}_1 and/or \tilde{t}_1 are lighter than the gluino, tend to allow for a top or bottom squark much lighter than 500 GeV while for the gluino and the squarks from the first two generations the lower bounds are almost touching 500 GeV and 1 TeV, respectively.

Thus, at a time when dedicated search for the squarks from the third generation would be on, while other strongly interacting superpartners still remaining unreachable, the preparedness to decipher the most from a positive signal would be something of genuine priority. There have been some studies in the past [32, 33] where techniques of measuring masses of the squarks from the third generation were discussed in scenarios where these squarks are produced in the decays of gluino. In particular, these studies suggested studying the edge structure of the m_{tb} distribution when gluino decays to $t b \chi_1^{+/-}$ through a light stop or sbottom. Further, in recent times, phenomenology of stop as the next to lightest supersymmetric particle (NLSP) has been considered at the LHC and/or Tevatron in scenarios like Gauge Mediated SUSY Breaking (GMSB) [34] or the CMSSM [35]. Interesting studies of probing the third generation squark sector, in particular, the stop sector through the study of the Higgs bosons were taken up in Refs. [36, 37].

Once we know about the primary quantities like the production cross sections of these SUSY particles and their masses, we would turn to learn about their couplings. These, together, would be reflective of the amount of chiral admixtures present in the mass eigenstates of the bottom and the top squarks. Dedicated study in this area is not abound, particularly in the context of LHC. However, a rather recent work [38] put the issue in perspective with the top squark sector in reference. Further, there are recent works [39, 40] proposing new techniques to reconstruct the top squark by tagging the top quarks.

As we will see in the next section, the observables in the sbottom and the stop sectors, particularly the basic ones like the masses and the mixings, are controlled by some parameters which are common to both. Incidentally, some of them also control the compositions of the charginos and the neutralinos in an important way. Thus, it is only natural to expect some reasonable correlations inherent in these sectors. Such correlations might provide some phenomenological handle in systematic explorations of these sectors in tandem and this is what we like to address here.

In this work, we perform a case-study with the production of the lighter bottom squark

at the 14 TeV LHC which eventually decays either to a top squark and a SM W^\pm boson or to a lighter chargino and a top quark or to a bottom quark along with a neutralino. Note that the first of these decay modes is the only one that involves squarks from both sbottom and the stop sectors and thus could reflect on the simultaneous features of these two sectors, i.e., the so-called entanglement. Note that the decay $\tilde{b}_1 \rightarrow \tilde{t}_1 W^+$ boson would be significantly enhanced only if both of the squarks have significant $SU(2)$ (left) admixtures. This decay mode was first discussed in Ref.[41]. In this work, we point out that this is where the entanglement between the sbottom and the stop sectors is likely to play an important role.

For all the decay modes mentioned above, the resulting final states would contain b -jets; either from the direct decays of the bottom squark or from the subsequent decays of the top squark or the top quark. It was also noted in Ref.[41] that the p_T spectrum of the b quarks, the W^\pm -bosons and the missing p_T spectra could be different for the above decay modes. Thus, the count of events enriched with bottom quarks, W^\pm bosons and missing p_T with characteristic kinematic properties could be indicative of the mixing-pattern present in the sbottom and stop sectors. We also point out that the LHC running at 7 TeV is not likely to offer much insight in such a study.

The paper is organised as follows. In section 2, we briefly outline the roles of different SUSY parameters that control the masses and the mixings in the sbottom and the stop sectors. We indicate how some of these parameters affect the compositions of the charginos and the neutralinos. We also touch upon the kind of correlation these common parameters might bring into the combined system. In section 3, we discuss the signals and the potential backgrounds at the LHC. A brief account of the setup and our analysis followed by the important observations are presented in section 4. In section 5, we summarise.

2 Masses and mixings

In this section, we outline the correlated nature of the system comprised of the third generation squarks and, to a varied extent, the charginos and the neutralinos.

The mass-squared matrix for the squarks, more relevantly, those from the third generation has the following generic form in the $(m_{\tilde{Q}_{3L}}, m_{\tilde{q}_{3R}})$ basis:

$$M_{\tilde{q}_3}^2 = \begin{pmatrix} m_{LL}^2 + m_{q_3}^2 & m_{q_3} m_{LR} \\ m_{q_3} m_{LR} & m_{RR}^2 + m_{q_3}^2 \end{pmatrix} \quad (1)$$

where

$$\begin{aligned} m_{LL}^2 &= m_{\tilde{Q}_{3L}}^2 + (T_3 - e \sin^2 \theta_W) m_Z^2 \cos 2\beta \\ m_{RR}^2 &= m_{\tilde{q}_{3R}}^2 + e \sin^2 \theta_W m_Z^2 \cos 2\beta \\ m_{LR}^2 &= A_{q_3} - \mu R \end{aligned} \quad (2)$$

where m_{q_3} is the bottom or the top quark mass, $m_{\tilde{Q}_{3L}}$ ($m_{\tilde{q}_{3R}}$) is the SUSY-breaking soft mass for the left (right)-chiral bottom or the top squark, T_3 and e are the isospin quantum

number and the electric charge of the squark in context, θ_W is the Weinberg angle and A_{q_3} is the soft SUSY breaking scalar trilinear parameter that appears in the scalar potential of the MSSM (A_b or A_t , as the case may be). R is equal to $\tan \beta$ ($\cot \beta$) for the sbottom (stop) sector. The second term in each of the first two expressions of equation (2) is proportional to $m_Z^2 \cos 2\beta$ and are known as the $SU(2)_L$ and $U(1)_Y$ D -terms originating in the quartic term of the scalar potential.

Further, let us write down the general formula for the mass eigenvalues of the physical states obtained on mixing of the chiral degrees of freedom:

$$m_{(\tilde{b}, \tilde{t})_{(1,2)}}^2 = \frac{1}{2} \left(2m_{b,t}^2 + m_{LL}^2 + m_{RR}^2 \mp \sqrt{(m_{LL}^2 - m_{RR}^2)^2 + 4m_{LR}^2 m_{b,t}^2} \right) \quad (3)$$

where the subscript 1(2) on the left hand side corresponds to the negative (positive) sign in front of the term under square-root on the right thus ensuring the mass-variable with subscript 1 (2) is the lighter (heavier) of the two mass eigenstates. The expressions involving the mixing angles are as follows:

$$\begin{aligned} \cos \theta_{\tilde{b}, \tilde{t}} &= \frac{-m_{b,t} m_{LR}}{\sqrt{m_{b,t}^2 m_{LR}^2 + (m_{b_1, \tilde{t}_1}^2 - m_{LL}^2)^2}} \\ \sin \theta_{\tilde{b}, \tilde{t}} &= \frac{m_{LL}^2 - m_{b_1, \tilde{t}_1}^2}{\sqrt{m_{b,t}^2 m_{LR}^2 + (m_{b_1, \tilde{t}_1}^2 - m_{LL}^2)^2}}. \end{aligned} \quad (4)$$

The lighter mass eigenstates in terms of the mixing angles have the general form:

$$\begin{aligned} \tilde{t}_1 &= \cos \theta_{\tilde{t}} \tilde{t}_L + \sin \theta_{\tilde{t}} \tilde{t}_R \\ \tilde{b}_1 &= \cos \theta_{\tilde{b}} \tilde{b}_L + \sin \theta_{\tilde{b}} \tilde{b}_R \end{aligned} \quad (5)$$

while the heavier ones are orthogonal states, respectively. Note that $0 < \theta_{\tilde{b}, \tilde{t}} < \pi$ by convention. Also, under this convention, a mass eigenstate is purely left-chiral in nature for $\theta_{\tilde{b}, \tilde{t}} = 0^\circ$ and entirely right-chiral when $\theta_{\tilde{b}, \tilde{t}} = 90^\circ$. A detailed description of this sector can be found in the thesis work of Ref.[42].

A key issue which we like to exploit here in this work is that the soft mass for the left-chiral degrees of freedom ($m_{\tilde{Q}_{3L}}$) is common to both sbottom and stop sectors. The sole difference between the two sectors in this part arises due to the so-called D -term contributions which are different for the two members of the isospin-doublet ($m_{\tilde{t}_L}$ and $m_{\tilde{b}_L}$). On the other hand, $m_{\tilde{q}_{3R}}$ for the two sectors can be different ($m_{\tilde{t}_R}$ and $m_{\tilde{b}_R}$, respectively) as these correspond to isospin singlets not related by any symmetry.

A few important points pertinent to the present study that emerge from equations (1), (2) and (3) are as follows. Clearly, through its presence in the off-diagonal terms of the mass-squared matrices, μ controls the mixings, *i.e.*, the chiral contents of the mass eigenstates, provided the trilinear couplings are not too large. Also, note that μ appears as a product with $\tan \beta$ (in the sbottom sector) or $\cot \beta$ (in the stop sector). Hence, choice of $\tan \beta$ as a basic parameter could determine the role of μ by tempering the product-term

up to an order of magnitude over the range $5 < \tan \beta < 50$. The patterns of such mixings are effectively captured, in a somewhat global way, in the parametrisation of Ref.[43] in terms of a ratio of the diagonal and the off-diagonal entries in the mass-square matrix. It can be easily checked that for $A_t (A_b) \ll \mu \cot \beta (\mu \tan \beta)$, the off-diagonal terms in the two sectors are comparable when $\tan \beta \approx 6$ which is uniquely determined by the ratio m_t/m_b . Thus, in a situation where the diagonal terms of the mass matrices for these two sectors are comparable, the role of μ in determining the mixing would be similar under such circumstances, for any value of μ .

Further, it is to be noted that the relative values of the soft masses $m_{\tilde{Q}_{3L}}$ and $m_{\tilde{q}_{3R}}$ appearing in the diagonal terms of the mass-squared matrix influence the chiral contents of the sbottom and the stop mass eigenstates in a definitive way in the presence of mixing. For example, maximal mixing in the top (bottom) squark sector requires $m_{\tilde{t}_L}(\tilde{b}_L) \approx m_{\tilde{t}_R}(m_{\tilde{b}_R})$ at the weak scale. This is a robust, but rather intuitive, requirement. Larger the off-diagonal term is, larger a deviation from the equality of these masses can be afforded for obtaining maximal mixing. Thus, assuming that the off-diagonal terms of the mass-squared matrices in both the sectors are likely to be primarily controlled by the corresponding fermion masses, almost near equality of the soft chiral masses in the sbottom sector is required to yield close to maximal mixing. By the same token, for the stop sector, a somewhat larger difference in the chiral soft masses can still result in a large mixing for given values of $A_{b,t}$, μ and $\tan \beta$.

However, such near equalities are *unlikely* to be achieved in generic high scale scenarios with universal scalar masses (including mSUGRA) and with a grand desert between the high scale and the electroweak scale. Take for example, an $SO(10)$ GUT inspired scenario with a universal scalar mass m_0 [44] where the $SO(10)$ breaks directly to the SM gauge group at the GUT scale. Both left and right top squarks leave in the same 5-plet of the $SU(5)$ embedded in $SO(10)$. This would lead to (up to effects from physics above the GUT scale) $m_{\tilde{t}_L} = m_{\tilde{t}_R}$ at the GUT scale. It immediately follows that $m_{\tilde{t}_R} < m_{\tilde{t}_L}$ at the weak scale due to renormalisation group (RG) running. In contrast, $m_{\tilde{b}_R}$ can be different from $m_{\tilde{b}_L}$ at the high scale since \tilde{b}_L and \tilde{b}_R reside in different multiplets of $SO(10)$. Hence, at the weak scale, $m_{\tilde{b}_L}$ and $m_{\tilde{b}_R}$ can have any relative hierarchy if nonuniversality in scalar masses at some high scale is allowed for. Thus, in particular GUT motivated scenarios, the chiral contents of the sbottom mass eigenstates may vary in a more relaxed fashion unlike those of the stop mass eigenstates.

Thus, while maximal mixing in the sbottom sector can somewhat more naturally be achieved by fulfilling the requirement $m_{\tilde{b}_L} \approx m_{\tilde{b}_R}$, the same in the top squark sector can hardly be realized in popular GUT motivated scenarios that assume universal scalar masses at the high (unification) scale and the presence of a ‘grand desert’ between the latter and the weak scale. In other words, observation of maximal mixing in the stop sector could very well indicate a departure from this popular paradigm. In this work, we try to exploit this issue. Thus, we adopt a purely phenomenological approach. We vary the chiral soft masses in the stop sector freely to explore the mixing in this sector and its implications.

On the other side of the story, the values of the soft masses of the $U(1)$ and $SU(2)$ gauginos (M_1 and M_2), with respect to μ , are crucial for the masses and the compositions of the charginos and the neutralinos (their gaugino and higgsino contents) which, in turn, broadly dictate the phenomenology involving them. Note that the charginos and the neutralinos interact with sbottom and stop eigenstates with both gaugino and higgsino components they have. This immediately hints towards a possible bridge that μ could provide between the two sectors. In addition, the role of μ can be seen in conjunction with that of $\tan\beta$ in the stop and sbottom sector (as explained above) while the role of the latter in the chargino and the neutralino sectors could assume importance under specific situations. An illustrative study to this end encompassing both the sectors is beyond the scope of the present work and will be taken up in a subsequent study [45].

In this work we restrict ourselves to the study of possible correlations that might be present in the sbottom and the stop sectors. Such correlations are likely to be best manifested in studies where both sectors have explicit involvements. The most significant of such situations could be realised in the productions of the lighter sbottom (lighter stop) at the colliders followed by its decays to the stop (sbottom) where W^\pm -bosons appear. We thus focus on a particular case of production of bottom squarks at the LHC followed by their subsequent decays with an aim to study the imprints of mixings in the involved sectors.

3 The Signal and the Background

In this section we present some aspects of phenomenology of the lighter of the bottom squarks at the LHC. Recently, in the context of a SUSY/MSSM ‘golden region’ [46, 47], such a study was taken up in Ref.[48]. This was necessarily limited, though in a rather motivated way, to a low μ regime with all the squarks from the first two generations taken to be rather heavy. The study stuck to an appropriate final state. In the present study, for our purpose, we adopt a rather open approach and analyse other possible final states originating from sbottom production at the LHC. This, as we will see, would inevitably involve the top squarks and thus may potentially shed light into the chiral compositions of the bottom and the top squarks in a correlated way. As discussed in the Introduction, this might even have reference to the texture of the gaugino sector in the same go.

Unlike in Ref.[48] where only pair-production of bottom squarks was considered, we keep the options open for other production processes which may eventually lead to a pair of bottom squarks at the LHC. These include production of a lighter bottom squark in association with a gluino and pair-production of gluinos where a gluino may decay subsequently to a bottom quark and an sbottom. These three modes of lighter sbottom production are shown schematically below:

- $pp \rightarrow \tilde{b}_1 \tilde{b}_1^*, \tilde{b}_1 \tilde{b}_1, \tilde{b}_1^* \tilde{b}_1^*$
- $pp \rightarrow \tilde{g} \tilde{b}_1, \tilde{g} \tilde{b}_1^* : \tilde{g} \rightarrow b \tilde{b}_1^*, \bar{b} \tilde{b}_1$

- $pp \rightarrow \tilde{g}\tilde{g} : \tilde{g} \rightarrow b\tilde{b}_1^*, \bar{b}\tilde{b}_1$

Now, an sbottom would always lead to a bottom quark in its decay, be it from a direct decay or through top quark production under a cascade. These are illustrated below.

- $\tilde{b}_1 \rightarrow b\chi_{i=1-4}^0$
- $\tilde{b}_1 \rightarrow t\chi_{j=1,2}^-$
- $\tilde{b}_1 \rightarrow \tilde{t}_1 W^- : \tilde{t}_1 \rightarrow b\chi_j^+, t\chi_i^0$

Note that any of these modes could lead to at least a pair of lighter bottom squarks and up to four bottom quarks (in the case of gluino pair-production) in the final state.

As indicated above, the bottom squark may have different possible decay modes out of which the ones to $\tilde{t}_1 W^\pm$, $t\chi_1^\pm$, $b\chi_1^0$ and $b\chi_2^0$ would be of importance. As for \tilde{t}_1 , its decays to $t\chi_1^0$, $t\chi_2^0$, $b\chi_1^\pm$ would be in context. Further, the gauge bosons (like W^\pm), the charginos and the neutralinos all would contribute to both leptonic and hadronic final states. In fact, as pointed out in the Introduction, the decay channels $\tilde{b}_1 \rightarrow \tilde{t}_1 W^\pm$ and $\tilde{b}_1 \rightarrow t\chi_1^\pm$ could lead to identical final states. Hence, if the branchings in these two channels are complementary in nature, rates for the final state events may not be much sensitive to the variation of the same. Thus, they may not shed much light on the couplings (and hence, on the mixings angles) involved. We will get back to this issue in the next section where we study situations under which clearer imprints of branchings and hence mixing angles are left in the events rates of the different final states. We would also contrast those to a generic scenario where all decay modes of \tilde{b}_1 are open and some of them are significant.

It is clear from the above discussion that the multiplicities of bottom quarks in the final state, at the parton-level, may vary between 2 and 4. While an experimental study of final states even with a moderate bottom quark multiplicity is a challenging proposition, their presence, nonetheless, would boost the counts for low-multiplicity (up to 2) final states through enhanced combinatoric factors. With these general possibilities in mind, we pick a benchmark (reference) MSSM spectrum in the next section for our subsequent analysis.

The final states we consider are the following:

1. $2 \text{ } b\text{-jets} + \geq 4 \text{ jets} + \geq 1\text{-lepton} + \cancel{E}_T$
2. $2 \text{ } b\text{-jets} + \geq 4 \text{ jets} + \text{same-sign dilepton (SSDL) pair} + \cancel{E}_T$
3. $2 \text{ } b\text{-jets} + \geq 4 \text{ jets} + \text{opposite-sign dilepton (OSDL) pair} + \cancel{E}_T$

where by leptons only the electrons and the muons are meant. The first of these final state has been studied in Ref.[48] as mentioned in the beginning of this section. In our case, this remains to be an important channel for two reasons: first, because the presence of a lepton in the final state helps negotiate the otherwise large pure QCD background and second, because it is less suppressed compared to dilepton final states indicated above. However, as expected, for the dilepton final states the backgrounds are further suppressed thus making them worthy of a closer study. In addition, there is always the well-known advantage of studying signals in multiple channels which, when studied simultaneously, may potentially shed light on intricate issues pertaining to the mass-spectrum and the involved couplings in a more efficient and definitive way.

As for the backgrounds for the final states indicated above, we considered several SM processes that could be potentially strong. These are $Zt\bar{t}+0, 1, 2, 3 \text{ jets}$, $Wt\bar{t}+0, 1, 2, 3 \text{ jets}$, $t\bar{t}+3, 4 \text{ jets}$, $tbW+0, 1 \text{ jets}$. Note that $t\bar{t}$ -pair production and the same with extra hard jets in low multiplicity (up to 2 extra jets) are unlikely to yield serious background because of the minimum lepton and jet multiplicities we required for our signal. Fakes from charm and light quark jets are not taken into account in this study.

4 The Setup and the Analysis

The setup for our analysis is based on two ‘benchmark’ scenarios about which variations are studied. These consist of two sets of weak-scale MSSM input parameters arranged in a minimalistic way for the purpose. These would be sufficient to demonstrate the goals of the present study. The first one is shown in Table 1. This explores the prospect of a heavier spectrum where the masses of the gluino and that of the squarks from the first two generations are somewhere near or just exceeding their present bounds in conformity with recent studies at the LHC and their interpretations within the much relaxed 19-dimensional pMSSM framework [29]. The second benchmark scenario is elaborated in Table 2. This, in turn, represents a lighter spectrum with somewhat lighter squarks from the third generation along with lighter gluino, charginos and neutralinos that are still very much allowed by the LHC data, as explained later in this section.

In addition, for these two spectra, we ensure compatibility with other experimental constraints like the lower bound on the mass of the lighter chargino obtained from the LEP experiments (≈ 105 GeV) and those pertaining to the anomalous muon magnetic moment ($a_\mu = \frac{g_\mu - 2}{2}$) [49, 50] and the rare Flavour Changing Neutral Current (FCNC) process like $b \rightarrow s\gamma$ [51, 52] while choosing these benchmark points. In fact, the observations in the latter two experiments, when considered in conjunction, favour $\mu > 0$ [53]. This is why we choose to work with positive values of μ in the present study. As for the SM-like lightest SUSY Higgs boson, we require a somewhat relaxed lower bound of 111 GeV as against the actual LEP constraint of 114.4 GeV [54, 55]. This relaxed bound is consistent with the more precise estimation [56, 57] of theoretical uncertainty involved in predicting the mass of the Higgs boson³.

As indicated in the Introduction, our goal is to work with a somewhat light bottom squark which is expected to be within the reach of LHC running at its design centre of mass energy, i.e., 14 TeV. Moreover, for our purposes, such a sbottom should have enough phase space to decay into a top squark along with a W boson. The probability of such a

³Strict compliance to the LEP Higgs bound and other precision observables like a_μ and $\text{BR}[b \rightarrow s\gamma]$ are enforced only to these reference points. Everywhere else, where the purpose is to explore the sensitivity of the event rates to the mixing angles, we just generated the combinations of these angles by varying the relevant MSSM inputs without worrying about their compatibility with these experimental observations.

decay would then be maximised when both \tilde{b}_1 and \tilde{t}_1 have substantial *left* chiral ($SU(2)$) admixture. However, by requiring such an admixture in them, it is impossible to achieve a mass-splitting of $\Delta m_{\tilde{b}_1 \tilde{t}_1} \sim \Delta m_{\tilde{b}_L \tilde{t}_L} \geq m_W$ between these two states. This is because, in such a limit, their masses at the weak scale are related, and at the lowest order, differ only by an $SU(2)$ D -term which is anyway not large (see equation (2), first expression). Hence, a compromise is needed and chiral mixings are to be allowed for. This would then definitely suppress the coupling $\tilde{b}_1 \tilde{t}_1 W^\pm$ but at the same time open up the required phase space for the decay $\tilde{b}_1 \rightarrow \tilde{t}_1 W^\pm$ to take place.

Parameters	Input values	Output spectrum
Gaugino masses (in GeV)	$M_1 = 200$ $M_2 = 400$ $M_3 = 1200$	$m_{\chi_1^0} \approx 198$ $m_{\chi_2^0} \approx 403$ $m_{\chi_1^\pm} \approx 403$ $m_{\tilde{g}} \approx 1193$
Chiral Squark masses (1st and 2nd generations) (in GeV)	$m_{\tilde{q}_{L,R}^{1,2}} = 1000$	$m_{\tilde{q}_{L,R}^{1,2}} \approx 1005 - 1010$
Third generation chiral squark masses (in GeV) and Mixing Angles	$m_{\tilde{Q}_{3L}} = 700$ $m_{\tilde{b}_R} = 1000$ $m_{\tilde{t}_R} = 500$	$m_{\tilde{b}_1} \approx 709$ $m_{\tilde{b}_2} \approx 1014$ $\theta_{\tilde{b}} = 1.9^\circ$ $m_{\tilde{t}_1} \approx 455$ $m_{\tilde{t}_2} \approx 757$ $\theta_{\tilde{t}} = 67^\circ$
Slepton Masses (in GeV)	$m_{\tilde{\ell}_{L,R}} = 600$	$m_{\tilde{\ell}} \approx 600$
A -parameters (in GeV)	$A_b = 0$ $A_t = -800$	— —
m_A (in GeV) μ (in GeV) $\tan \beta$	500 700 10	$m_{\chi_3^0} \approx 699$ $m_{\chi_4^0} \approx 711$ $m_{\chi_2^\pm} \approx 711$

Table 1: A somewhat *heavy* benchmark SUSY spectrum and the weak-scale values of the MSSM input parameters used to obtain the same. The input soft mass of the CP-odd Higgs is taken to be 500 GeV. The SUSY spectrum generator used for the purpose is Suspect v2.31. Throughout the analysis $m_{top} = 172.5$ GeV is used. Note that $m_{\tilde{q}} < m_{\tilde{g}}$.

In Table 1 we collect the set of relevant MSSM input parameters for the high-mass reference point and the resulting output spectrum that conform with the setup described above. We call this the high-mass benchmark point/spectrum. Note that the mixing angle in the sbottom sector, $\theta_{\tilde{b}}$ is rather small thus making the lighter sbottom an almost pure left

chiral state. However, $\theta_{\tilde{t}}$ is around 67° and hence it has some (15%) left chiral admixture. By varying the relevant MSSM inputs about their benchmark values, the mixing in the top squark sector can be significantly altered. This would affect the decay branching fractions of the bottom squark. As we would see later in this section, this can have some impact on the signatures at the LHC.

Parameters	Input values	Output spectrum
Gaugino masses (in GeV)	$M_1 = 100$ $M_2 = 200$ $M_3 = 600$	$m_{\chi_1^0} \approx 100$ $m_{\chi_2^0} \approx 207$ $m_{\chi_1^\pm} \approx 207$ $m_{\tilde{g}} \approx 655$
Chiral Squark masses (1st and 2nd generations) (in GeV)	$m_{\tilde{q}_{L,R}^{1,2}} = 1000$	$m_{\tilde{q}_{L,R}^{1,2}} \approx 1005 - 1010$
Third generation chiral squark masses (in GeV) and Mixing Angles	$m_{\tilde{Q}_{3L}} = 480$ $m_{\tilde{b}_R} = 700$ $m_{\tilde{t}_R} = 390$	$m_{\tilde{b}_1} \approx 500$ $m_{\tilde{b}_2} \approx 715$ $\theta_{\tilde{b}} = 4.3^\circ$ $m_{\tilde{t}_1} \approx 349$ $m_{\tilde{t}_2} \approx 571$ $\theta_{\tilde{t}} = 57.3^\circ$
Slepton Masses (in GeV)	$m_{\tilde{\ell}_{L,R}} = 600$	$m_{\tilde{\ell}} \approx 600$
A -parameters (in GeV)	$A_b = 0$ $A_t = -500$	— —
m_A (in GeV) μ (in GeV) $\tan \beta$	500 850 10	$m_{\chi_3^0} \approx 845$ $m_{\chi_4^0} \approx 849$ $m_{\chi_2^\pm} \approx 850$

Table 2: Same as in Table 1 except for a somewhat *smaller* masses for the lighter charginos and neutralinos, the gluino and the third generation squarks. Note that $m_{\tilde{q}} > m_{\tilde{g}}$.

To decide on the benchmark spectrum with lighter masses (Table 2), a closer look at recent LHC studies [7, 8, 9, 19] is warranted. These analyses discuss signals with heavy flavour jets (b -jets) and large missing transverse energy without [8] and with [9] an isolated lepton (e and/or μ). There, either \tilde{b}_1 [8] or \tilde{t}_1 [9] are assumed to be the lightest squark and the branching fractions of gluino decaying into them (in the respective cases) is 100%. Thus, in these studies, \tilde{b}_1 -s or \tilde{t}_1 -s are produced either directly in pairs or via production and subsequent decays of gluino. Further, it is assumed in these experimental studies that \tilde{b}_1 and \tilde{t}_1 always decay in specific channels, i.e., $\text{BR}[\tilde{b}_1 \rightarrow b\chi_1^0]$ [8] and $\text{BR}[\tilde{t}_1 \rightarrow b\chi_1^+]$ [9] are 100% in the respective cases. Ref.[8] rules out $m_{\tilde{g}} < 720$ GeV for $m_{\tilde{b}_1} < 600$ GeV. Ref.[9]

excludes $m_{\tilde{g}} < 500 - 520$ GeV for $m_{\tilde{t}_1}$ between 125 GeV and 300 GeV. In Ref.[9], exclusion limit is also placed on the $m_{\tilde{g}} - m_{\chi_1^0}$ plane when \tilde{t}_1 is still the lightest of the squarks but is heavy enough ($m_{\tilde{g}} < m_{\tilde{t}_1} + m_t$) such that \tilde{g} cannot decay into an on-shell \tilde{t}_1 and it decays via off-shell \tilde{t}_1 to $t\bar{t}\chi_1^0$ final state with a decay branching fraction of 100%. The analysis excluded $m_{\chi_1^0} < 40(80)$ GeV for $m_{\tilde{g}} < 570(540)$ GeV. All these reported exclusions are at 95% confidence level.

However, the above limits may be considered conservative because they assume the $\text{Br}[\tilde{g} \rightarrow \tilde{b}_1\bar{b} + h.c.]$ or $\text{Br}[\tilde{g} \rightarrow \tilde{t}_1\bar{t} + h.c.]$ to be 100%. In a situation where there is more than one third-generation squark lighter than the gluino, this assumption would not hold and may result in relaxed bounds. In addition, note that events from direct stop pair production are reported [9] to have a very low acceptance; presumably due to hard kinematic cuts used in the analysis. These issues may very well dilute the sensitivities of these experimental analyses (to a given data-set) which would eventually lower the exclusion limits. In Table 2, we tried to exploit this caveat to our advantage and settled on a somewhat lower mass for the gluino (≈ 655 GeV) in relation to $m_{\tilde{b}_1}$ (≈ 500 GeV) considered.

For the two benchmark scenarios, we work in an otherwise unconstrained SUSY scenario except retaining an imprint of unification of gaugino masses (at a high scale) in the choice of their weak scale values. Note, however, that such a choice is only to keep the analysis tractable and does not feature an essential part of our study. As is well-known, departure from such an assumption, can easily have nontrivial phenomenological implications. Two such examples are discussed in the context of the benchmark scenarios, the emphasis being on the subtle handles these may provide in the analysis and interpretation of the collider signals. A systematic study of the implications of such departures is beyond the scope of the present study though and would be taken up elsewhere [45].

In Table 3 we collect the lowest order cross sections for the strong-production processes that lead to a pair of \tilde{b}_1 , *viz.*, $pp \rightarrow \tilde{b}_1\tilde{b}_1^*, \tilde{b}_1\tilde{b}_1 + h.c., \tilde{b}_1\tilde{g} + h.c., \tilde{g}\tilde{g}$ for the 14 TeV run of the LHC. The cross sections are calculated by the event generator Pythia v6.420 [58] and cross-checked with CalcHEP v2.5.4 [59]. Note that this is a conservative estimate since the next to leading order (NLO) contribution from QCD to squark (including stop and sbottom) and gluino productions [60, 61, 62] and the same combined with next to leading log (NLL) resummed soft-gluon contribution [63, 64] may increase the cross sections by $\sim 30 - 40\%$ on an average, for our benchmark scenarios, the NLL contributions being far more important for the case of gluino and squarks from the first two generations. Two sets of cross sections are presented for the two benchmark spectra of Table 1 and Table 2. As expected, the respective cross sections are much larger for the lighter spectrum of Table 2. Also, in both cases the relative magnitudes of \tilde{g} -pair cross section are significant. So, if there is a reasonable branching fraction for the decay $\tilde{g} \rightarrow \tilde{b}_1\bar{b} + h.c.$, pair-production of gluino could become a useful source of \tilde{b}_1 -pair [32, 33].

The high-mass scenario (of Table 1) with $m_{\tilde{q}_{1,2}} < m_{\tilde{g}}$ turns out to be a rather conservative one. First and foremost, the individual cross sections for all the contributing processes

Spectrum	$\sigma_{\tilde{b}_1\tilde{b}_1}$ (pb)	$\sigma_{\tilde{b}_1\tilde{g}}$ (pb)	$\sigma_{\tilde{g}\tilde{g}}$ (pb)
Table 1 ($m_{\tilde{q}_{1,2}} < m_{\tilde{g}}$)	0.030	0.003	0.022
Table 2 ($m_{\tilde{q}_{1,2}} > m_{\tilde{g}}$)	0.265	0.110	1.764

Table 3: Lowest order production cross sections at the LHC ($\sqrt{s} = 14$ TeV) for different strong production processes that lead to pair of lighter bottom squarks using the mass-spectra of Tables 1 and 2. CTEQ6L parton distribution function is used with renormalisation/factorisation scale set at $\sqrt{\hat{s}}$.

are on the smaller side because the sparticles are heavier. Second, the branching ratio for $\tilde{g} \rightarrow \tilde{b}_1 b$ is affected since $\tilde{g} \rightarrow \tilde{q}_{1,2} q (+h.c.)$ is kinematically accessible and when summed over 4 flavours, would become dominant. Third, we miss out on potential contributions from the production of $\tilde{q}_{1,2}$, in pair or in association with a gluino, which could have led up to 4 bottom quarks had the hierarchy been $m_{\tilde{t}_1} < m_{\tilde{b}_1} < m_{\tilde{g}} < m_{\tilde{q}_{1,2}} \sim m_{\tilde{b}_2} \sim m_{\tilde{t}_2}$.

The suppression of $\text{Br}[\tilde{g} \rightarrow \tilde{b}_1 b + \text{h.c.}]$ is demonstrated in the upper part of Table 4 for the heavy spectrum of Table 1. It is, however, a straight-forward exercise to find out to what extent $\text{Br}[\tilde{g} \rightarrow \tilde{b}_1 b + \text{h.c.}]$ may get enhanced if the mass-hierarchy of the gluino and the squarks from the first two generations is flipped, other parameter remaining the same. Note that the ratio of the branching fractions of the gluino to \tilde{b}_1 and \tilde{t}_1 (i.e., 9.8 : 13.1) reflects the the ratio of the decay widths of the gluino in these two modes. Thus, when only these two modes add up to 100% of the branching fraction, $\text{Br}[\tilde{g} \rightarrow \tilde{b}_1 \bar{b} + h.c.]$ would be around 43.5%. More importantly, such tweaking of the squark-masses would immediately bring in further contributions from heavier squarks when they decay into gluino followed by the latter decaying into \tilde{b}_1 . In contrast, our choice of low-mass spectrum of Table 2 represents a favourable scenario on all respective counts laid down above. It is evident from the lower parts of Tables 3 and 4 that the low-mass benchmark spectrum boosts both cross sections and its branching fractions relevant for our purpose. Thus, the two benchmark scenarios are arranged to demonstrate the extremal situations.

Table 4 also collects the branching fractions of \tilde{b}_1 and \tilde{t}_1 to different modes that are instrumental for the study we undertake. For the high-mass spectrum, we see that the crucial mode $\tilde{b}_1 \rightarrow W^- \tilde{t}_1$ has a reasonable branching fraction of about 64%. For the low-

Spectrum	Branching fractions \tilde{q} and/or \tilde{g} -decay (in %)	Branching fractions \tilde{b}_1 -decay (in %)	Branching fractions \tilde{t}_1 -decay (in %)
Table 1 (heavier masses) $m_{\tilde{g}} > m_{\tilde{q}_{1,2}} > m_{\tilde{b}_1} > m_{\tilde{t}_1}$	$\tilde{g} \rightarrow b\tilde{b}_1^* + \tilde{b}\tilde{b}_1 : 9.8$ $\tilde{g} \rightarrow t\tilde{t}_1^* + \tilde{t}\tilde{t}_1 : 13.1$ $\tilde{g} \rightarrow q\tilde{q}^* + \tilde{q}\tilde{q} : 77.1$	$\tilde{b}_1 \rightarrow W^-\tilde{t}_1 : 64.1$ $\tilde{b}_1 \rightarrow t\chi_1^- : 19.6$ $\tilde{b}_1 \rightarrow b\chi_2^0 : 15.1$ $\tilde{b}_1 \rightarrow b\chi_1^0 : 1.2$	$\tilde{t}_1 \rightarrow t\chi_1^0 : 87.0$ $\tilde{t}_1 \rightarrow b\chi_1^+ : 13.0$
Table 2 (lighter masses) $m_{\tilde{q}_{1,2}} > m_{\tilde{g}} > m_{\tilde{b}_1} > m_{\tilde{t}_1}$	$\tilde{q}_R \rightarrow q\tilde{g} : 95.0$ $\tilde{q}_L \rightarrow q\tilde{g} : 70.0$ $\tilde{g} \rightarrow b\tilde{b}_1^* + \tilde{b}\tilde{b}_1 : 48.5$ $\tilde{g} \rightarrow t\tilde{t}_1^* + \tilde{t}\tilde{t}_1 : 51.5$	$\tilde{b}_1 \rightarrow W^-\tilde{t}_1 : 34.5$ $\tilde{b}_1 \rightarrow t\chi_1^- : 36.2$ $\tilde{b}_1 \rightarrow b\chi_2^0 : 27.7$ $\tilde{b}_1 \rightarrow b\chi_1^0 : 1.6$	$\tilde{t}_1 \rightarrow t\chi_1^0 : 39.2$ $\tilde{t}_1 \rightarrow b\chi_1^+ : 60.8$

Table 4: Branching fractions of \tilde{g} , \tilde{b}_1 and \tilde{t}_1 for the mass-spectra given in Tables 1 and 2.

mass spectrum, this branching fraction drops to around 34%, presumably due to a combined effect of diminished splitting between \tilde{b}_1 and \tilde{t}_1 and possible enhancements of the competing modes. This is a plausible explanation since, as can be seen from Tables 1 and 2, the left ($SU(2)$) admixtures in \tilde{b}_1 and \tilde{t}_1 are not different in these two cases.

One of the goals of this work is to understand how sensitive the event rates in different leptonic final states are to the mixing angles in the third generation squark sector. As pointed out earlier, since all the relevant leptonic final states get contributions from almost all possible branching modes in this sector, our ability to filter out the individual contributions to the extent possible would help extract information on the mixing angles involved.

Towards this end one needs to know how sensitive the individual branching fractions of the bottom and the top squarks are to the variations of the mixing angles $\theta_{\tilde{b}}$ and $\theta_{\tilde{t}}$. We choose to study the effect of variation of $\theta_{\tilde{t}}$ only. The reason behind this is two-fold. First, $\theta_{\tilde{t}}$ is more sensitive to small variations in the SUSY inputs than $\theta_{\tilde{b}}$ thanks to the amplifying SM factor m_t sitting in the off-diagonal term of the corresponding mass-squared matrix. Second, $\theta_{\tilde{t}}$ variation directly affects the branching fraction of \tilde{t}_1 . Nonetheless, an analogous study with respect to $\theta_{\tilde{b}}$ would have its own characteristics though effecting a comparable variation on it would require major tweaking of the soft parameters of the bottom squark sector.

At this stage, for such a study to be meaningful, it is to be necessarily assumed that the

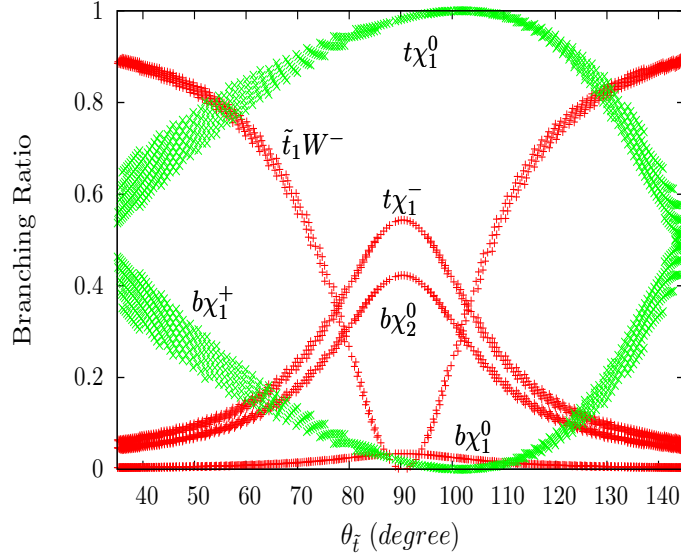


Figure 1: (a) Variations of branching fractions of the lighter bottom squark (red/dark grey band) and lighter top squark into different major decay modes as a function of $\theta_{\tilde{t}}$ while keeping $m_{\tilde{t}_1}$ within the range 445–465 GeV. The variation of $\theta_{\tilde{t}}$ is achieved (see Figure 2) by varying the soft parameters $m_{\tilde{t}_R}$ and A_t while keeping all other parameters relevant to the third generation squarks fixed at the benchmark values.

masses of the lighter sbottom and the lighter stop are already known from the experiments. This ensures that the concerned kinematics remain mostly unaltered for the relevant production and decay processes. Thus, we vary $m_{\tilde{t}_R}$ and A_t to achieve the variation in $\theta_{\tilde{t}}$ while allowing $m_{\tilde{t}_1}$ to vary only within a certain range (± 10 GeV) about the reference value of $m_{\tilde{t}_1} = 455$ GeV (see Table 1). Clearly, such variations do not at all alter either the mass of the lighter bottom squark or the mixing angle in that sector. We also keep μ , $\tan\beta$, M_1 and M_2 fixed during this variation so that the masses and the mixings in the chargino and the neutralino sectors remain almost fixed in the process. Altogether, this ensures that the variations we see in the branching fractions of the bottom and the top squarks are almost entirely due to the variation in $\theta_{\tilde{t}}$. This would definitely help obtain a clearer picture of the role of $\theta_{\tilde{t}}$ in shaping the pattern of cascade decays of the lighter sbottom.

In Figure 1, we present the variation of branching fractions of both \tilde{b}_1 and \tilde{t}_1 as functions of $\theta_{\tilde{t}}$. Note that the products of different branching fractions of these excitations determine the predominance of certain cascade-patterns when they decay. In the present case, the possible decay mode of lighter sbottom to lighter stop and charged Higgs boson is closed, the latter being rather heavy (resulting from our choice of an input m_A of 500 GeV).

Out of the decay widths that enter the calculation of the branching fractions of the lighter sbottom, only $\Gamma(\tilde{b}_1 \rightarrow \tilde{t}_1 W^-)$ depends upon $\theta_{\tilde{t}}$ and is actually proportional to $\cos^2 \theta_{\tilde{b}} \cos^2 \theta_{\tilde{t}}$ [41]. Thus, as a function of $\theta_{\tilde{t}}$, the variations of different sbottom branching fractions are solely determined by the branching profile of $\tilde{b}_1 \rightarrow \tilde{t}_1 W^-$ which goes as $\cos^2 \theta_{\tilde{t}}$ (and hence

the symmetry about $\theta_{\tilde{t}} = 90^\circ$), $\theta_{\tilde{b}}$ being held fixed, as is the case here⁴. Note that such a symmetry with respect to $\theta_{\tilde{t}}$ is not there in the variation of branching fractions of \tilde{t}_1 . This is because they have a somewhat complicated dependence on $\theta_{\tilde{t}}$. Clearly, this variation neither alters $m_{\tilde{b}_1}$ nor $\theta_{\tilde{b}}$. Thus, \tilde{b}_1 remains to be almost purely left chiral.

It is to be noted that the variations in Figure 1 are in the form of bands. The reason behind this is that the variation of $\theta_{\tilde{t}}$ is achieved by simultaneous variations of $m_{\tilde{t}_R}$ and A_t over the ranges $300 \text{ GeV} \leq m_{\tilde{t}_R} \leq 1500 \text{ GeV}$ and $-3 \text{ TeV} \leq A_t \leq +3 \text{ TeV}$, respectively while ensuring $m_{\tilde{t}_1}$ to be roughly in the range $445 \leq m_{\tilde{t}_1} \leq 465 \text{ GeV}$.

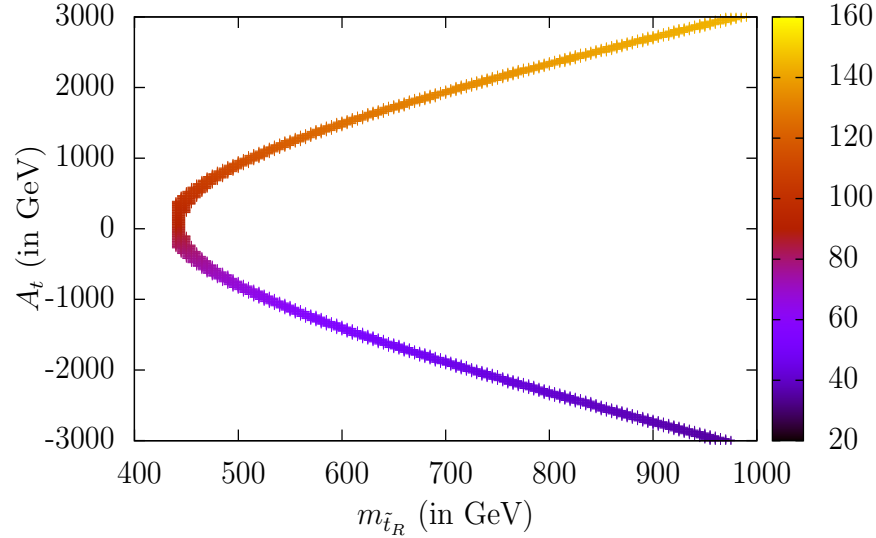


Figure 2: Ranges of $\theta_{\tilde{t}}$ in degrees presented in colour-code (for the setup in Figure 1) as $m_{\tilde{t}_R}$ and A_t vary keeping $445 \text{ GeV} < m_{\tilde{t}_1} < 465 \text{ GeV}$. $m_{\tilde{Q}_{3L}}$ and $m_{\tilde{b}_R}$ are kept fixed at 700 GeV and 1000 GeV, respectively.

Figure 2 reflects some important features relevant for the phenomenology under the given setup. These are:

- The graph is almost symmetric about $A_t = 0$. This is expected when A_t dominates in the off-diagonal term of the stop mass-squared matrix. Given that $\tan \beta = 10$ and $\mu = 700 \text{ GeV}$ for our case and the off-diagonal term dominates over most of the A_t -range studied above.
- The above issue is equivalent to having complementary angles and this is clearly seen in the figure.

⁴In fact, while the left branch with $\theta_{\tilde{t}} < 90^\circ$ arises for $A_t < 0$, the right one with $\theta_{\tilde{t}} > 90^\circ$ results from $A_t > 0$. Also, moving away on both sides from $\theta_{\tilde{t}} = 90^\circ$, i.e., increasing amount of mixing, corresponds to increasing $|A_t|$. Since, with increasing $|A_t|$, mixing is dominantly determined by A_t , it is expected that further one is from $\theta_{\tilde{t}} = 90^\circ$ on either side of the curve, it is more likely that similar values of $|A_t|$ result in similar values of branching fractions.

- The resulting band is rather narrow. This is because we require $m_{\tilde{t}_1}$ be within the range $445 \text{ GeV} < m_{\tilde{t}_1} < 465 \text{ GeV}$.
- For values of $m_{\tilde{t}_R}$ much larger than $m_{\tilde{Q}_{3L}}$ one requires large values of $|A_t|$ for bringing down $m_{\tilde{t}_1}$ to the mentioned range. The resulting mixing can be close to maximal or lower but never reaches very small values (corresponding to dominance of left-chiral admixture).
- Maximal mixings (around 45° and 135°) are expected for $m_{\tilde{t}_R}$ in the vicinity of $m_{\tilde{Q}_{3L}}$. However, as mentioned earlier, since the mixing in the stop sector is driven by m_t , A_t plays a crucial role in mixing and help achieve close to maximal mixing even when $m_{\tilde{t}_R}$ is somewhat away from $m_{\tilde{Q}_{3L}}$. This is clear from the bluish-purple and yellowish-orange bands extended over the range $700 \text{ GeV} < m_{\tilde{t}_R} < 850 \text{ GeV}$.
- For smaller values of $m_{\tilde{t}_R}$ ($\gtrsim 450 \text{ GeV}$), $m_{\tilde{t}_1}$ required by us is close to these values. Hence, for this range, \tilde{t}_1 is almost purely right-chiral ($\theta_{\tilde{t}} \simeq 90^\circ$). No mixing is required for the purpose and hence A_t values are seen to be within a couple of hundred GeVs.

The problem is now to understand if the imprints of these branching fractions can be read out by studying suitable final states at the LHC. As indicated earlier, this is going to be rather challenging given that the third generation squarks all lead to very similar final states. Thus, disentangling individual contributions (read, contaminations), which is so necessary to unravel the sector, is a complicated proposition. This is more so since, in a bottom-rich environment, identifying multiple bottom quarks could very well hold the key.

To simulate SUSY events we use the event generator Pythia v6.420 [58]. Pythia is interfaced with the framework SUSYHIT [65] that in turn uses the SLHA [66] protocol to integrate Suspect 2.31 [67], the popular SUSY mass-spectrum generator and SDECAY [68] and HDECAY [69] which calculate the decay branching fractions of the SUSY particles and the Higgs bosons respectively. To simulate the SM backgrounds discussed in section 3, partonic events are generated with Alpgen v2.13 [70] We have used CTEQ6L [71] parametrisation of the parton distribution function (PDF) via Pythia's interface to LHAPDF v5.7 [72]. The renormalisation/factorisation scale is set to $\sqrt{\hat{s}}$, for both signal and background analyses. In case of background processes in Alpgen for which $\sqrt{\hat{s}}$ is not available as a choice for the renormalisation/factorisation scale, the default option for the same is used. To attempt a somewhat realistic treatment of the final state objects like jets, leptons, photons and the missing transverse energy we interfaced AcerDET v1.0 [73] as the fast detector simulator.

Unweighted events for the signal processes from Pythia and that for the SM background processes from Alpgen are then showered using Pythia with initial and final state radiations on. To avoid possible double-counting, multijet events from the Matrix Element (ME) calculation in Alpgen are matched with the jets from the Parton Shower (PS) using the MLM prescription [74], available in Alpgen as the default. In the entire exercise, a jet is defined with a minimum clustered energy in the calorimeter of 25 GeV having a cone size

of $\Delta R = 0.4$ within $|\eta| \leq 2.5$.

For a jet to be triggered as a b -jet, it is required to have $p_T > 5$ GeV within $|\eta| < 2.5$ and an isolation from a neighbouring jet of $\Delta R < 0.2$ is required. Further, an average tagging efficiency of 50% is used for the b -jets.

Electrons and muons are triggered in AcerDET only if they have $p_T > 5$ GeV, $|\eta| < 2.4$ and have a lepton-jet separation $\Delta R_{\ell j} > 0.4$. Further, to ensure the purity of the candidates, energy deposited within a cone of radius $\Delta R < 0.2$ about the candidate lepton was required to be within 10 GeV.

We incorporate a generic set of kinematic cuts in our analysis following ATLAS [75]. The requirements for the final state objects and the employed cuts are as follows:

- Two tagged b -jets (with a b -tagging efficiency of 50%), both with $p_T > 40$ GeV.
- At least four jets with the hardest one requiring $p_T^j > 100$ GeV and the other three with $p_T^j > 50$ GeV. On top of this, for an inclusive jet final state all jets should have $p_T^{jet} > 40$ GeV.
- For inclusive 1-lepton and SSDL final states, isolated leptons with $p_T^\ell > 20$ GeV are required. For OSDL final state a, both leptons are required to have $p_T^\ell > 10$ GeV. Also, for the SSDL and OSDL final states two and only two leptons are required.
- missing $\cancel{E}_T > 150$ GeV,

On top the above set of cuts, we use cuts on two more kinematic variables which help reduce the SM background in an effective way. The first one is the so-called *transverse mass* of the system comprised of the lepton(s) and missing energy and defined as

$$M_T = \sqrt{(E_T^\ell + \cancel{E}_T)^2 - (p_x^\ell + \cancel{p}_x)^2 - (p_y^\ell + \cancel{p}_y)^2}.$$

Traditionally used to reconstruct a leptonically decaying W -boson, a suitable cut on M_T thus could efficiently reduce the W -boson background from the SM processes. In the left panel of Figure 3 we show the M_T distributions for the two benchmark scenarios of Tables 1 and 2 and that for the SM background combined over all the contributing processes. The m_T profile for the SM background (the profile in light-green) nose-dives beyond 100 GeV with a subdominant tail extending up to 500 GeV. For the signal, the one for the high-mass case (in yellow) and the low-mass one (in blue) extend to 550 GeV and 650 GeV, respectively. As we can see, a cut of $M_T > 200$ GeV would efficiently eliminate the SM background where W bosons are associated.

It is also known that the variable called effective mass (M_{eff}) where

$$M_{eff} = \sum_{jets} p_T^j + \sum_{leptons} p_T^\ell + \cancel{E}_T$$

can also be a powerful generic discriminator in search of new physics with highly massive exotic states. In the right panel of Figure 3 we illustrate the M_{eff} distributions for the

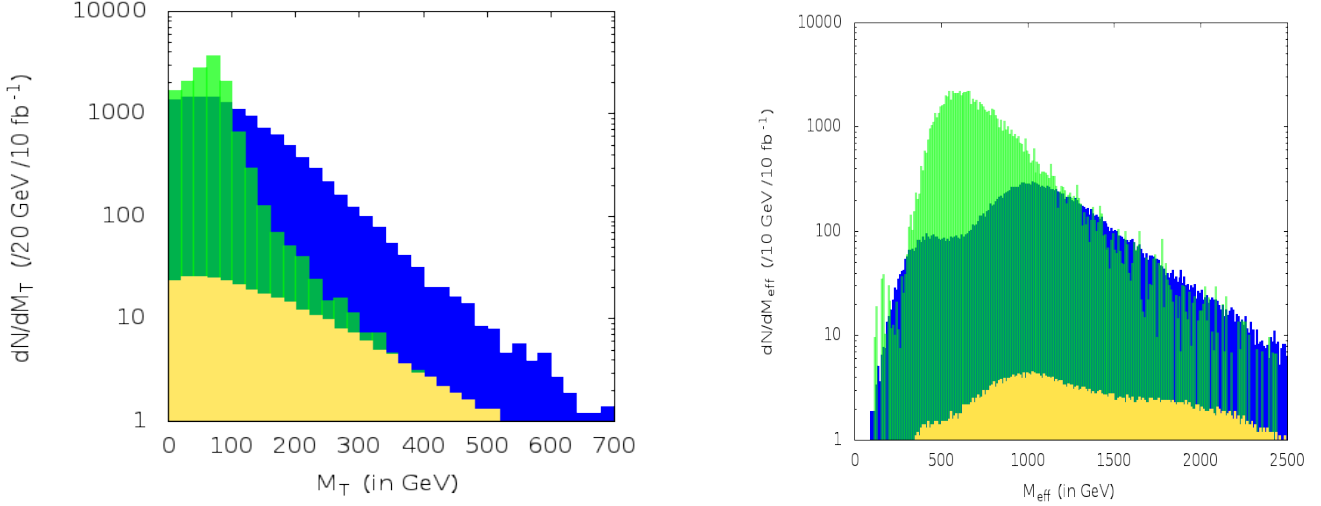


Figure 3: The transverse mass (left) and the effective mass (right) spectra for the summed-up background (in light green/light grey) and the signal. The profile at the bottom in yellow/ash is for the signal in the high-mass benchmark scenario of Table 1. The profile in blue/black is for the signal in the low-mass benchmark scenario of Table 2.

signal and the SM background as described for the M_T curves and following the same colour convention. Studying the trends of the distributions in this plot, we require a flat minimum of 800 GeV for M_{eff} for analysing both high and low mass benchmark scenarios. In the latter case, it seems to be a little overkill though. However, we stick to this particular value to bring uniformity in the overall analysis (the SM background thus remaining the same) which indeed may render this part of the study only conservative.

In the subsequent part of this section we demonstrate how the event counts for different final states vary not only as a function of $\theta_{\tilde{t}}$ but also when $\theta_{\tilde{b}}$ is varied while $m_{\tilde{t}_1}$ and $m_{\tilde{t}_2}$ are held fixed within ± 10 GeV of the corresponding benchmark values. In all these cases we incorporated the kinematic cuts and the b -tagging efficiency as mentioned above.

The variations in the mixing angles are effected by simultaneously tweaking $m_{\tilde{Q}_{3L}}, m_{\tilde{t}_R}, m_{\tilde{b}_R}$ and A_t . The change in rates in different multi-lepton and jet final states reflect the sensitivity of the rates to varying mixing angles, masses being held fixed. For this, we again take the spectra of Tables 1 and 2 as the reference ones with somewhat higher and lower squark masses, respectively.

In Table 5 we present the different event rates for the high-mass scenario of Table 1. Note that the benchmark scenario here is chosen in a way such that $\theta_{\tilde{t}} \approx 67^\circ$ which means the mixing angle is halfway between the maximal (45°) and what corresponds to a purely right-handed \tilde{t}_1 (90°). To be precise, $\theta_{\tilde{t}} = 67^\circ$ refers to about a 15% admixture of \tilde{t}_L in

\tilde{t}_1 . The mixing in the sbottom sector remains practically fixed at a rather low angle ($\approx 2^\circ$) thus rendering \tilde{b}_1 to be almost purely left-chiral.

$\theta_{\tilde{t}}, \theta_{\tilde{b}}$	$\text{BR}[\tilde{b}_1 \rightarrow \tilde{t}_1 W^-]$	$2b + \geq 4j + \cancel{E}_T$ $\geq 1\ell$	$2b + \geq 4j + \cancel{E}_T$ $+ \text{OSDL}$	$2b + \geq 4j + \cancel{E}_T$ $+ \text{SSDL}$
$25.1^\circ, 4.7^\circ$ $\tilde{t}_1^{L_{max}}, \tilde{b}_1^L$	89.4 %	66	11	4
$46.6^\circ, 46.0^\circ$ $\tilde{t}_1^{LR}, \tilde{b}_1^{LR}$	78.8 %	74	15	5
$33.5^\circ, 83.0^\circ$ $\tilde{t}_1^{L_{max}}, \tilde{b}_1^R$	45.5 %	48	7	2
From Table 1 $67.0^\circ, 1.9^\circ$ $\tilde{t}_1^{LR}, \tilde{b}_1^L$	64.0 %	65	14	4
$84.7^\circ, 2.6^\circ$ $\tilde{t}_1^R, \tilde{b}_1^L$	9.4 %	58	9	3
$87.9^\circ, 87.2^\circ$ $\tilde{t}_1^R, \tilde{b}_1^R$	0.0 %	27	3	0
SM Background	-	12	4	0

Table 5: Variations of events rates (for the spectrum in Table 1) in different leptonic final states containing two tagged b -jets along with other light quark jets and missing transverse energy with different combinations of $\theta_{\tilde{t}}$ and $\theta_{\tilde{b}}$. The kinematic cuts used are as discussed in the text. The event-rates correspond to an accumulated luminosity of 300 fb^{-1} and an average b -tagging efficiency of 50%. The last row presents the summed-up events rates from various SM backgrounds (see text for details) for the respective final states under the same set of cuts.

In the first column of Table 5, the mixing angles in the stop and the sbottom sectors are presented along with the corresponding chiral contents of \tilde{t}_1 and \tilde{b}_1 . The suffix LR on \tilde{t}_1 and \tilde{b}_1 indicates that these mass eigenstates have some significant L and R contaminations while either L or R as a suffix indicates that these are either almost purely left- or right-chiral in nature, respectively. It is important to note the mixing angles in the first column in this Table. These combinations of angles are again obtained by varying $m_{\tilde{Q}_{3L}}, m_{\tilde{b}_R}, m_{\tilde{t}_R}, A_t$ and A_b while holding $m_{\tilde{t}_1}$ and $m_{\tilde{b}_1}$ within $\pm 10 \text{ GeV}$ of the respective benchmark values. Same procedure is taken for subsequent Tables in this section. Although our intention has been to demonstrate the effect of different combinations of mixing angles in the sbottom and the stop sectors spanning over purely left-chiral pairs to right-chiral ones passing through intermediate situations, we cannot really realise a situation when both \tilde{b}_1 and \tilde{t}_1 are almost

pure left-chiral states and still allowing for the necessary splitting between $m_{\tilde{b}_1}$ and $m_{\tilde{t}_1}$. The reason is quite clear and is as follows. Since both \tilde{b}_L and \tilde{t}_L are states determined by \tilde{Q}_{3_L} , the mass-eigenstates \tilde{b}_1 and \tilde{t}_1 dominated respectively by them are bound to be rather degenerate ($\sim m_{\tilde{Q}_{3_L}}$). The only splitting between them is due to the $SU(2)$ D -term ($\propto m_Z^2 \cos 2\beta$) originating from the different electroweak (isospin (T_3), electric charge) quantum numbers the left-chiral states carry. The splitting between $m_{\tilde{b}_1}$ and $m_{\tilde{t}_1}$ (i.e., the one that ensures $m_{\tilde{b}_1} > m_{\tilde{t}_1} + W$) that we are particularly interested in, in the present study, is thus not achievable unless we allow for some mixing in the top squark sector. This is what is reflected in the first row of Table 5. The angle $\theta_{\tilde{t}} \approx 24.7^\circ$ indicates that \tilde{t}_1 has some right-chiral admixture but still dominated (since, $\theta_{\tilde{t}} < 45^\circ$) by the left-chiral state. This observation would have ramifications beyond the present context. It implies that given a mass-splitting between \tilde{b}_1 and \tilde{t}_1 , combination of arbitrarily small $\theta_{\tilde{b}}$ and $\theta_{\tilde{t}}$ (i.e., arbitrarily large *left* chiral components in both \tilde{b}_1 and \tilde{t}_1) are not feasible. This is true even when we minimally supersymmetrise the SM without subjecting it to further constraints. This is a kind of entanglement we like to point out. In other words, the phenomenon rules out the possibility of having a full-strength coupling in the on-shell decay $\tilde{b}_1 \rightarrow \tilde{t}_1 W$ (or, for that matter, $\tilde{t}_1 \rightarrow \tilde{b}_1 W$, for a reverse hierarchy of masses between \tilde{t}_1 and \tilde{b}_1).

From Table 5 it can be seen that the variations in the event counts of different leptonic final states as the combination of mixing angles vary are anything but drastic. This is not unexpected. The reason behind this is that when the branching fraction of $\tilde{b}_1 \rightarrow \tilde{t}_1 W$ decreases, the same in other decay modes, e.g., $\tilde{b}_1 \rightarrow t\chi_1^{+/-}$ and $\tilde{b}_1 \rightarrow b\chi_2^0$, start increasing (see Figure 1). The decay width for $\tilde{b}_1 \rightarrow \tilde{t}_1 W$ could be directly affected by double suppression from both $\theta_{\tilde{b}}$ and $\theta_{\tilde{t}}$ at the same time while its other modes of decay only see $\theta_{\tilde{b}}$ directly. Thus, there can be a possible sharing of branching fractions among these modes all of which contribute to the leptonic final states discussed here. Hence, we may reasonably expect a less drastic variation of the event counts with varying $\theta_{\tilde{b}}$ and $\theta_{\tilde{t}}$ when these modes are open.

Thus, an appropriate setup to improve the sensitivity to the mixing angles and hence to see the tell-tale signatures of the variations of mixing angles on the event rates of various multilepton final states is to have a situation when the decay modes $\tilde{b}_1 \rightarrow t\chi_1^{+/-}$ and $\tilde{b}_1 \rightarrow b\chi_2^0$ are kinematically closed. This we realise by making M_2 larger than $m_{\tilde{b}_1}$ ($M_2 = 750$ GeV) so that the lighter chargino and the second lightest neutralino becomes heavier than \tilde{b}_1 . We also set $\mu = 1$ TeV (changing it from 750 GeV, as was for the benchmark scenario of Table 5) so that the compositions of the chargino and the neutralino sectors remain more or less unchanged.

The resulting variations are presented in Table 6. Branching fractions are now only shared between the decay modes $\tilde{b}_1 \rightarrow \tilde{t}_1 W$ and $\tilde{b}_1 \rightarrow b\chi_1^0$. Events from these two decay modes could, to a good extent, may unambiguously tell us about the respective decay branching fractions which, in turn, would be indicative of the mixing angles involved. However, $\tilde{b}_1 \rightarrow b\chi_1^0$ would lead to leptonically quiet events with b -jets and \cancel{E}_T which are hard

to identify over the huge SM background, particularly damaging one being of QCD origin with ‘fake’ b -jets. Thus, one needs to concentrate on how the rates in different multilepton final states are varying to get an idea about the mixing angle(s) in the sbottom and stop sectors. The combinations of angles are kept close to the corresponding ones of Table 5. As we can see, the branching fractions to $\tilde{t}_1 W$ mode, shown in column 2, displays a much clearer variation with the angle-combinations when compared to Table 5. With increasing right-chiral component in both \tilde{b}_1 and \tilde{t}_1 , the branching fraction $\tilde{b}_1 \rightarrow \tilde{t}_1 W$ gets diminished straight-away. Note that this decay mode of sbottom is the only source of leptons from \tilde{b}_1 down the cascade. The other one being $\tilde{b}_1 \rightarrow b\chi_1^0$, this would only lead to b -jets and missing energy in the final state. Thus, a more drastic (compared to Table 5 decrease in the number of events in different leptonic final states is expected as right chiral components increase. This is exactly what Table 6 indicates.

$\theta_{\tilde{t}}, \theta_{\tilde{b}}$	$\text{BR}[\tilde{b}_1 \rightarrow \tilde{t}_1 W^-]$	$2b + \geq 4j + \cancel{E}_T$ $+ \geq 1\ell$	$2b + \geq 4j + \cancel{E}_T$ $+ \text{OSDL}$	$2b + \geq 4j + \cancel{E}_T$ $+ \text{SSDL}$
$24.7^\circ, 2.1^\circ$ $\tilde{t}_1^{L_{\max}}, \tilde{b}_1^L$	99.7 %	47	9	4
$45.6^\circ, 44.8^\circ$ $\tilde{t}_1^{LR}, \tilde{b}_1^{LR}$	97.1 %	49	10	4
$39.4^\circ, 87.2^\circ$ $\tilde{t}_1^{L_{\max}}, \tilde{b}_1^R$	9.9 %	10	1	0
$88.5^\circ, 2.8^\circ$ $\tilde{t}_1^R, \tilde{b}_1^L$	27.8 %	16	3	0
$89.2^\circ, 87.5^\circ$ $\tilde{t}_1^R, \tilde{b}_1^R$	0.0 %	7	1	0
SM Background	-	12	4	0

Table 6: The same variations as shown in Table 5 but with nonuniversal gaugino masses where for \tilde{b}_1 , only the modes $\tilde{b}_1 \rightarrow \tilde{t}_1 W$ and $b\chi_1^0$ are open. Except for $M_2 = 750$ GeV and $\mu = 1$ TeV all other parameters are as there in Table 1.

In both Tables 5 and 6, the rates for both OSDL and SSDL final states are found to be on the lower side compared to the inclusive 1-lepton case. This is quite expected since final states with more number of leptons involve further suppression due to added leptonic branching. The combined SM backgrounds for the respective final states are indicated in the last rows of both the Tables. As can be gleaned from these numbers, except for the cases where both \tilde{b}_1 and \tilde{t}_1 have significant right-chiral components, the rates in the inclusive 1-lepton final state has significance above 5σ at an accumulated luminosity of 300 fb^{-1} . On the other hand, only the OSDL rate with both \tilde{t}_1 and \tilde{b}_1 having maximal possible

left-chiral contamination (i.e., $\tilde{t}_1^{LR}, \tilde{b}_1^L$ combinations in the first row) passes the 5σ mark⁵ at 300 fb^{-1} . The signal rates in the SSDL mode are indeed low throughout. However, since the SM background for this can be virtually eliminated, seeing a few events would suffice. Note that, at this stage, even a two fold increase in the accumulated luminosity is not going to change the overall situation drastically, at least qualitatively, except for the fact that we may have then a handful of very clean SSDL events. The bottom-line of Table 6 is that there could be a clear imprint of the product of $\cos\theta_{\tilde{b}}$ and $\cos\theta_{\tilde{t}}$ in the absolute and mutually relative rates of these leptonic final states, though at a somewhat high integrated luminosity. Thus, the corresponding mass value of the sbottom squark (around 700 GeV, along with the gluino of 1200 GeV) lives on the edge of explorability for such a study. This prompts us to take up an exactly similar study but now with a low-lying spectrum benchmarked in Table 2 and its non-universal (in terms of gaugino mass relationship) variant.

In Tables 7 and 8 we present studies which exactly emulate the proceedings of Tables 5 and 6, respectively but using the spectrum of Table 2. With $m_{\tilde{b}_1} \approx 500 \text{ GeV}$ and $m_{\tilde{g}} \approx 650 \text{ GeV}$, we definitely expect a larger yield of events in any given final state. That the numbers presented in both Tables 7 and 8 are of the same order as for their high-mass counterparts of Tables 5 and 6, reflects the fact that the former Tables have numbers for a much lower integrated luminosity of only 30 fb^{-1} as compared to 300 fb^{-1} for the latter ones. SM backgrounds also get scaled down by this luminosity factor. Tables 7 and 8 clearly demonstrate how the sensitivities to mixing angles can be better studied with lower masses of the involved SUSY particles for all the final states discussed.

The results presented in Tables 7 and 8 have direct correspondences to their high-mass counterparts presented in Tables 5 and 6. Note that, in Tables 6 and 8, even when both \tilde{t}_1 and \tilde{b}_1 are both almost purely right chiral, there are still significant number of leptonic (in particular, inclusive one-lepton events) events present, which is not quite expected had $\tilde{b}_1 \rightarrow \tilde{t}_1 W$ been the sole source of leptons in the final state. In fact, in our simulation not only \tilde{b}_1 -pairs but also $\tilde{g}\tilde{g}$ and $\tilde{g}\tilde{b}_1$ pairs are included, as pointed out in the beginning of section 3. Thus, most of the leptons, under such a circumstance, are coming from top-squarks produced in the decay of the gluino along with the ones from the decay of SM top quark obtained under the SUSY cascade. This brings us to an important issue.

Of particular interest is the cascade $\tilde{b}_1 \rightarrow \tilde{t}_1 W^- \rightarrow t \chi_1^0 W^- \rightarrow b W^+ \chi_1^0 W^- \rightarrow b + \text{leptons and/or jets} + \cancel{E}_T$. Here, note that the decay of a single \tilde{b}_1 gives rise to two W -bosons (with opposite charges): one coming directly from the decay of \tilde{b}_1 while the other appearing in the decay of a top quark (originating from a top squark) further down the cascade. Thus, if both \tilde{b}_1 -s undergo such a cascade, at some stage there would be four (4) W bosons there. Possibility of identifying more of them could provide us with a remarkable handle to remove the above-mentioned ‘spurious’ leptons that do not originate in

⁵This assumes a Gaussian estimation of the significance. However, for some of these low yields a Poissonian treatment would be more appropriate. The main issue here, however, is to take a simple note of the depleting counts in the dilepton final states for an integrated luminosity of 300 fb^{-1} .

$\theta_{\tilde{t}}, \theta_{\tilde{b}}$	$\text{BR}[\tilde{b}_1 \rightarrow \tilde{t}_1 W^-]$	$2b + \geq 4j + \cancel{E}_T$ $\geq 1\ell$	$2b + \geq 4j + \cancel{E}_T$ $+ \text{OSDL}$	$2b + \geq 4j + \cancel{E}_T$ $+ \text{SSDL}$
$31.4^\circ, 2.7^\circ$ $\tilde{t}_1^{L_{max}}, \tilde{b}_1^L$	57.1 %	36	12	4
$45.7^\circ, 47.7^\circ$ $\tilde{t}_1^{LR}, \tilde{b}_1^{LR}$	45.9 %	42	11	5
$32.3^\circ, 82.7^\circ$ $\tilde{t}_1^{L_{max}}, \tilde{b}_1^R$	16.6 %	32	8	1
From Table 2 $64.8^\circ, 2.7^\circ$ $\tilde{t}_1^{LR}, \tilde{b}_1^L$	29.4 %	46	11	5
$86.6^\circ, 3.2^\circ$ $\tilde{t}_1^R, \tilde{b}_1^L$	1.1 %	58	16	7
$79.7^\circ, 88.8^\circ$ $\tilde{t}_1^R, \tilde{b}_1^R$	0.0 %	38	10	3
SM Background	-	1	0	0

Table 7: Variations of events rates (for the spectrum in Table 2) in different leptonic final states containing two tagged b -jets along with other light quark jets and missing transverse energy with different combinations of $\theta_{\tilde{t}}$ and $\theta_{\tilde{b}}$. The kinematic cuts used are as discussed in the text. The event-rates correspond to an accumulated luminosity of 30 fb^{-1} and an average b -tagging efficiency of 50%. The last row presents the summed-up events rates from various SM backgrounds (see text for details) for the respective final states under the same set of cuts.

the cascades of \tilde{b}_1 . Even the model-background originating from direct (in pairs) production of \tilde{t}_1 , which has not been considered in this work, can be removed if multiple W -s can be reconstructed in the final states discussed here. This would facilitate direct probe to the coupling $\tilde{b}_1 \tilde{t}_1 W$ thus reflecting on the mixings in the bottom and the top squark sectors.

To the best of our knowledge dedicated study in this line is still lacking. One can take useful cue from some recent studies on multi-top final states [76, 77, 78]. As pointed out in these works, reconstructing multiple top quarks is an inherently difficult proposition, particularly in the complex environment of the LHC where the final state objects overlap. However, identifying multiple W -bosons is not expected to be more complicated than tracking down multiple top quarks. This is because, identifying multiple top quarks involves successive reconstructions of first, W bosons and subsequently, the individual top quarks they are coming from. Also, note that with our choice of soft SUSY parameters, \tilde{t}_1 always decays to $t\chi_1^0$ thus making one of the W bosons in the cascade always coming from a top

$\theta_{\tilde{t}}, \theta_{\tilde{b}}$	$\text{BR}[\tilde{b}_1 \rightarrow \tilde{t}_1 W^-]$	$2b + \geq 4j + \cancel{E}_T$ $+ \geq 1\ell$	$2b + \geq 4j + \cancel{E}_T$ $+ \text{OSDL}$	$2b + \geq 4j + \cancel{E}_T$ $+ \text{SSDL}$
$34.9^\circ, 2.5^\circ$ $\tilde{t}_1^{L_{max}}, \tilde{b}_1^L$	97.8 %	75	24	5
$47.8^\circ, 47.3^\circ$ $\tilde{t}_1^{LR}, \tilde{b}_1^{LR}$	86.3 %	69	19	6
$32.3^\circ, 82.6^\circ$ $\tilde{t}_1^{L_{max}}, \tilde{b}_1^R$	20.1 %	51	12	5
$60.7^\circ, 2.9^\circ$ $\tilde{t}_1^{LR}, \tilde{b}_1^L$	94.9 %	73	22	7
$81.8^\circ, 2.5^\circ$ $\tilde{t}_1^R, \tilde{b}_1^L$	60.6 %	70	15	7
$80.8^\circ, 88.8^\circ$ $\tilde{t}_1^R, \tilde{b}_1^R$	0.0 %	44	9	3
SM Background	-	1	0	0

Table 8: The same variations as shown in Table 5 but with nonuniversal gaugino masses where for \tilde{b}_1 decay, only the modes $\tilde{b}_1 \rightarrow \tilde{t}_1 W$ and $b\chi_1^0$ are open. Except for $M_2 = 550$ GeV and $\mu = 700$ GeV, values of all other parameters are same as in Table 2.

quark. This may offer some degree of simplicity while undertaking a feasibility-study of exploring such a cascade. It can be foreseen that capability of identifying these W bosons would prove to be crucial in a generic scenario where \tilde{b}_1 can decay to other channels ($t\chi_1^{+/-}$, $b\chi_2^0$, for example) which ultimately give rise to identical final states.

5 Summary and Outlook

Physics analyses of recent LHC data hint essentially to super-TeV squarks from the first two generations and to a somewhat massive gluino. However, till now, the LHC experiments are not as sensitive to searches for the sbottom and the stop squarks. Consequently, much lighter sbottom and stop squarks are still allowed. This is exactly under such a situation when searches for them assume special significance.

In this work, we aim for a rather conservative approach. We presume a scenario where only the lightest of the bottom and top squarks have significant cross sections at the 14 TeV run of the LHC. Gluinos are taken to be intermediate in mass such that they could contribute to our final states only in a moderate way. On the other hand, squarks from the first two generations are considered to be heavier than a TeV following recent analyses.

These are, however, still within the reach of LHC with reasonable cross sections and are able to contribute to the final states considered by us in different ways. However, in the spirit of the present work, to be conservative, we neglected those contributions. The compulsion is then to learn from the limited, nonetheless crucial, piece of information offered through the squarks from the third generation.

It is pointed out that requiring some splitting between the the lighter sbottom and the stop eigenstates may set in some kind of an entanglement between the two sectors. This is because of the common left-chiral soft mass that enters the diagonal terms of the mass-squared matrices for both the sectors. One possible fall out of such entanglement is that the mixing angle in one of these sectors may constrain the corresponding one in the other sector. The degree of such entanglement may depend upon quite a few factors. The absolute masses of \tilde{b}_1 and \tilde{t}_1 and the splitting between these masses are two such important ones.

In this work we demonstrate the phenomenology of the lighter sbottom squark. The reference decay mode considered is $\tilde{b}_1 \rightarrow \tilde{t}_1 W$. This decay mode is naturally enhanced when both \tilde{b}_1 and \tilde{t}_1 have significant left-chiral content in them. Sensitivity of the resulting phenomenology to variations of the chiral contents of \tilde{b}_1 and \tilde{t}_1 would thus help probe their compositions. We point out the situations under which a clean study is possible. Under involved situations, we suggest that our ability to identify more number of W -bosons in the final state would hold the key. We also stress that observations in multiple final states naturally would facilitate understanding. We demonstrate the issue with somewhat heavy sbottom and stop followed by the lighter ones at the 14 TeV LHC run. For the heavier spectrum we required an integrated luminosity in the ballpark of 300 fb^{-1} while for the lighter spectrum 30 fb^{-1} may be good enough.

Maximally (even moderately) mixed top and bottom squarks is something outside the realm of much popular CMSSM/mSUGRA frameworks. Any hint of such mixings would firmly indicate departure from these scenarios. As exemplified in Tables 6 and 8, it may happen, that such a study may crucially bank on the nonuniversal masses in the gaugino sector thus exposing another crucial piece of information on the SUSY spectrum in the same go.

A further entanglement is envisaged between the chargino/neutralino sector and the sector comprising of the third generation squarks. Here, the common agents responsible are μ and $\tan\beta$. The role of μ in such entanglements is expected to be tempered by the value of $\tan\beta$ and hence could well be limited to scenarios with light stop and sbottom. Further, due to the opposite roles played by $\tan\beta$ in determining the mixings in the stop and sbottom sectors, sbottom sector may see somewhat larger correlation with the chargino/neutralino sector. It is important to note that since both mixings and masses in the latter sector are controlled (to different extents) by μ and $\tan\beta$, the entanglements can easily have both kinematic and dynamical implications. Moreover, with squarks from the third generations involved, they respond to both gaugino and higgsino components of the

charginos/neutralinos in characteristic ways under SUSY cascades.

In this work, we have not considered a substantial, positive higher order correction (at NLO or NLO+NLL combined) to the SUSY cross sections. Consideration of this, could increase the cross section significantly (by $\sim 35\%$) for our benchmark scenarios. However, to be conservative in our approach, and that we are unable to consistently treat the SM background on a similar footing, we postpone this to a future work. Further, we have not included possible contributions from \tilde{b}_2 and \tilde{t}_2 either from direct production or from cascades. The former can very well be small while contribution from the cascades may still be appreciable under favourable circumstances. Neither do we discuss a possible reverse hierarchy of $m_{\tilde{t}_1} > m_{\tilde{b}_1}$ where a similar phenomenology with stress on the decay $\tilde{t}_1 \rightarrow \tilde{b}_1 W$ can be studied. Also, a dedicated analysis could have been undertaken for the 7-TeV run of the LHC. Apriori, given that the cross sections for the processes relevant for such a study are much smaller at 7 TeV, only some legitimate low-lying spectra might be of interest. However, even in that case, the requirement for total integrated luminosity would be in the ballpark of $\lesssim 100 \text{ fb}^{-1}$ which the LHC is not foreseeing for its 7-TeV run.

Acknowledgements: The authors are partially supported by funding available from the Department of Atomic Energy, Government of India for the Regional Centre for Accelerator-based Particle Physics (RECAPP), Harish-Chandra Research Institute. AD likes to thank J-L Kneur, M. Muhlleitner and D. Zerwas for help in using the packages SUSPECT and SUSYHIT. Saurabh Niyogi likes to thank Sanjoy Biswas, Nishita Desai, Satyanarayan Mukhopadhyay for many useful discussions on physics and computational issues. Both AD and SN like to thank Amitava Datta for insightful discussions. The authors acknowledge the use of computational facility available at RECAPP and thank Joyanto Mitra for technical help.

References

- [1] G. Aad *et al.* [Atlas Collaboration], Phys. Rev. Lett. **106** (2011) 131802 [arXiv:1102.2357 [hep-ex]];
- [2] J. B. G. da Costa *et al.* [Atlas Collaboration], Phys. Lett. B **701** (2011) 186 [arXiv:1102.5290 [hep-ex]];
- [3] G. Aad *et al.* [ATLAS Collaboration], Eur. Phys. J. C **71**, 1647 (2011) [arXiv:1103.6208 [hep-ex]].
- [4] G. Aad *et al.* [ATLAS Collaboration], [arXiv:1103.6214 [hep-ex]].
- [5] G. Aad *et al.* [ATLAS Collaboration], arXiv:1109.6572 [hep-ex].
- [6] G. Aad *et al.* [ATLAS Collaboration], arXiv:1109.6606 [hep-ex].

- [7] G. Aad *et al.* [ATLAS Collaboration], Phys. Lett. B **701** (2011) 398 [arXiv:1103.4344 [hep-ex]].
- [8] ATLAS Collaboration, *Search for supersymmetry in pp collisions at $\sqrt{s} = 7\text{TeV}$ in final states with missing transverse momentum, b-jets and no leptons with the ATLAS detector*, ATLAS-CONF-2011-098.
- [9] ATLAS Collaboration, *Search for supersymmetry in pp collisions at $s = 7\text{TeV}$ in final states with missing transverse momentum, b-jets and one lepton with the ATLAS detector*, ATLAS-CONF-2011-130.
- [10] V. Khachatryan *et al.* [CMS Collaboration], Phys. Lett. B **698** (2011) 196 [arXiv:1101.1628 [hep-ex]].
- [11] S. Chatrchyan *et al.* [CMS Collaboration], arXiv:1107.1279 [hep-ex];
- [12] S. Chatrchyan *et al.* [CMS Collaboration], arXiv:1107.1870 [hep-ex];
- [13] S. Chatrchyan *et al.* [CMS Collaboration], [arXiv:1109.2352 [hep-ex]].
- [14] S. Chatrchyan *et al.* [CMS Collaboration], JHEP **1107** (2011) 113. [arXiv:1106.3272 [hep-ex]].
- [15] CMS Collaboration, *Search for supersymmetry in events with a lepton and missing energy*, CMS-PAS-SUS-11-015.
- [16] CMS Collaboration, *Search for supersymmetry in all-hadronic events with MT_2* , CMS-PAS-SUS-11-005.
- [17] CMS Collaboration, *Search for supersymmetry in all-hadronic events with missing energy*, CMS-PAS-SUS-11-004.
- [18] CMS Collaboration, *Search for supersymmetry in all-hadronic events with T* , CMS-PAS-SUS-11-003.
- [19] Henri Bachacou, *BSM Results from LHC*, talk given at Lepton-Photon 2011, Mumbai, 2011.
- [20] J. A. Conley, J. S. Gainer, J. L. Hewett, M. P. Le and T. G. Rizzo, arXiv:1009.2539 [hep-ph];
- [21] J. A. Conley, J. S. Gainer, J. L. Hewett, M. P. Le and T. G. Rizzo, arXiv:1103.1697 [hep-ph].
- [22] J. Alwall, P. Schuster, N. Toro, Phys. Rev. **D79** (2009) 075020. [arXiv:0810.3921 [hep-ph]].
- [23] D. S. M. Alves, E. Izaguirre and J. G. Wacker, arXiv:1102.5338 [hep-ph].
- [24] D. Alves, N. Arkani-Hamed, S. Arora, Y. Bai, M. Baumgart, J. Berger, M. Buckley, B. Butler *et al.*, [arXiv:1105.2838 [hep-ph]].

- [25] H. Baer, M. Drees, C. Kao, M. Nojiri, X. Tata, Phys. Rev. **D50** (1994) 2148-2163. [arXiv:hep-ph/9403307 [hep-ph]].
- [26] V. D. Barger, C. Kao, R. -J. Zhang, Phys. Lett. **B483** (2000) 184-190. [hep-ph/9911510].
- [27] H. Baer, P. Mercadante, X. Tata, Phys. Lett. **B475** (2000) 289-294. [hep-ph/9912494].
- [28] U. Chattopadhyay, A. Datta, A. Datta, A. Datta, D. P. Roy, Phys. Lett. **B493** (2000) 127-134. [hep-ph/0008228].
- [29] S. Sekmen *et al.*, arXiv:1109.5119 [hep-ph].
- [30] N. Desai, B. Mukhopadhyaya, Phys. Rev. **D80** (2009) 055019. [arXiv:0901.4883 [hep-ph]].
- [31] C. Brust, A. Katz, S. Lawrence and R. Sundrum, arXiv:1110.6670 [hep-ph].
- [32] J. Hisano, K. Kawagoe, R. Kitano and M. M. Nojiri, Phys. Rev. D **66** (2002) 115004 [arXiv:hep-ph/0204078].
- [33] J. Hisano, K. Kawagoe and M. M. Nojiri, Phys. Rev. D **68** (2003) 035007 [arXiv:hep-ph/0304214].
- [34] Y. Kats, D. Shih, JHEP **1108**, 049 (2011). [arXiv:1106.0030 [hep-ph]].
- [35] K. Huitu, L. Leinonen, J. Laamanen, [arXiv:1107.2128 [hep-ph]].
- [36] G. Belanger, F. Boudjema, K. Sridhar, Nucl. Phys. **B568** (2000) 3-39. [hep-ph/9904348].
- [37] R. Dermisek, I. Low, Phys. Rev. **D77** (2008) 035012. [hep-ph/0701235 [HEP-PH]].
- [38] K. Rolbiecki, J. Tattersall and G. Moortgat-Pick, Eur. Phys. J. C **71** (2011) 1517 [arXiv:0909.3196 [hep-ph]].
- [39] T. Plehn, M. Spannowsky, M. Takeuchi and D. Zerwas, JHEP **1010** (2010) 078 [arXiv:1006.2833 [hep-ph]].
- [40] T. Plehn, M. Spannowsky and M. Takeuchi, JHEP **1105** (2011) 135 [arXiv:1102.0557 [hep-ph]].
- [41] K. Hidaka and A. Bartl, Phys. Lett. B **501** (2001) 78 [arXiv:hep-ph/0012021].
- [42] S. Kraml, arXiv:hep-ph/9903257.
- [43] R. Demina, J. D. Lykken, K. T. Matchev and A. Nomerotski, Phys. Rev. D **62** (2000) 035011 [arXiv:hep-ph/9910275].
- [44] Y. Kawamura, H. Murayama and M. Yamaguchi, Phys. Rev. D **51** (1995) 1337 [arXiv:hep-ph/9406245].
- [45] Work in progress; Asesh Krishna Datta and Saurabh Niyogi.
- [46] M. Perelstein and C. Spethmann, JHEP **0704** (2007) 070 [arXiv:hep-ph/0702038].

- [47] M. Perelstein and C. Spethmann, arXiv:0710.4148 [hep-ph].
- [48] H. Li, W. Parker, Z. Si and S. Su, Eur. Phys. J. C **71** (2011) 1584 [arXiv:1009.6042 [hep-ph]].
- [49] S. P. Martin and J. D. Wells, Phys. Rev. D **64** (2001) 035003 [arXiv:hep-ph/0103067].
- [50] A. Djouadi, M. Drees and J. L. Kneur, JHEP **0603** (2006) 033 [arXiv:hep-ph/0602001].
- [51] F. Mahmoudi, Comput. Phys. Commun. **178** (2008) 745 [arXiv:0710.2067 [hep-ph]].
- [52] A. Arbey, M. Battaglia and F. Mahmoudi, arXiv:1110.3726 [hep-ph].
- [53] J. L. Feng and K. T. Matchev, Phys. Rev. Lett. **86** (2001) 3480 [arXiv:hep-ph/0102146].
- [54] R. Barate *et al.* [LEP Working Group for Higgs boson searches and ALEPH Collaboration and and], Phys. Lett. B **565** (2003) 61 [arXiv:hep-ex/0306033].
- [55] S. Schael *et al.* [ALEPH Collaboration and DELPHI Collaboration and L3 Collaboration and], Eur. Phys. J. C **47** (2006) 547 [arXiv:hep-ex/0602042].
- [56] G. Degrandi, S. Heinemeyer, W. Hollik, P. Slavich and G. Weiglein, Eur. Phys. J. C **28** (2003) 133 [arXiv:hep-ph/0212020].
- [57] S. Heinemeyer, Int. J. Mod. Phys. A **21** (2006) 2659 [arXiv:hep-ph/0407244].
- [58] T. Sjostrand, S. Mrenna, P. Z. Skands, JHEP **0605** (2006) 026. [hep-ph/0603175].
- [59] A. Pukhov, arXiv:hep-ph/0412191.
- [60] W. Beenakker, R. Hopker, M. Spira and P. M. Zerwas, Nucl. Phys. B **492** (1997) 51 [arXiv:hep-ph/9610490].
- [61] W. Beenakker, R. Hopker and M. Spira, arXiv:hep-ph/9611232; Also see the website,
`\protect\vrule width0pt\protect\href{http://www.thphys.uni-heidelberg.de/~plehn/i`
- [62] W. Beenakker, M. Kramer, T. Plehn, M. Spira and P. M. Zerwas, Nucl. Phys. B **515** (1998) 3 [arXiv:hep-ph/9710451].
- [63] W. Beenakker, S. Brensing, M. Kramer, A. Kulesza, E. Laenen and I. Niessen, JHEP **0912** (2009) 041 [arXiv:0909.4418 [hep-ph]].
- [64] W. Beenakker, S. Brensing, M. Kramer, A. Kulesza, E. Laenen and I. Niessen, JHEP **1008** (2010) 098 [arXiv:1006.4771 [hep-ph]].
- [65] A. Djouadi, M. M. Muhlleitner, M. Spira, Acta Phys. Polon. **B38** (2007) 635-644. [hep-ph/0609292].
- [66] B. C. Allanach, C. Balazs, G. Belanger, M. Bernhardt, F. Boudjema, D. Choudhury, K. Desch, U. Ellwanger *et al.*, Comput. Phys. Commun. **180** (2009) 8-25. [arXiv:0801.0045 [hep-ph]].
- [67] A. Djouadi, J. -L. Kneur, G. Moultaka, Comput. Phys. Commun. **176** (2007) 426-455. [hep-ph/0211331].

- [68] M. Muhlleitner, A. Djouadi, Y. Mambrini, Comput. Phys. Commun. **168** (2005) 46-70. [hep-ph/0311167].
- [69] A. Djouadi, J. Kalinowski, M. Spira, Comput. Phys. Commun. **108** (1998) 56-74. [hep-ph/9704448].
- [70] M. L. Mangano, M. Moretti, F. Piccinini, R. Pittau, A. D. Polosa, JHEP **0307** (2003) 001. [hep-ph/0206293]; see also an updated version (from 2006) of the manual distributed with the latest version of the package in its DOCS folder.
- [71] J. Pumplin, D. R. Stump, J. Huston, H. L. Lai, P. M. Nadolsky, W. K. Tung, JHEP **0207** (2002) 012. [hep-ph/0201195].
- [72] M. R. Whalley, D. Bourilkov, R. C. Group, “The Les Houches accord PDFs (LHAPDF) and LHAGLUE,” [hep-ph/0508110]; see also <http://hepforge.cedar.ac.uk/lhapdf/>.
- [73] E. Richter-Was, “AcerDET: A Particle level fast simulation and reconstruction package for phenomenological studies on high p(T) physics at LHC,” [hep-ph/0207355].
- [74] S. Hoeche, F. Krauss, N. Lavesson, L. Lonnblad, M. Mangano, A. Schalicke, S. Schumann, [hep-ph/0602031].
- [75] G. Aad *et al.* [The ATLAS Collaboration], arXiv:0901.0512 [hep-ex].
- [76] B. S. Acharya, P. Grajek, G. L. Kane, E. Kuflik, K. Suruliz and L. T. Wang, arXiv:0901.3367 [hep-ph].
- [77] G. Servant *et al.*, *Four top final states* in “New Physics at the LHC. A Les Houches Report: Physics at TeV Colliders 2009 - New Physics Working Group”, ed. G. Brooijmans *et al.* arXiv:1005.1229 [hep-ph].
- [78] G. Cacciapaglia, R. Chierici, A. Deandrea, L. Panizzi, S. Perries and S. Tosi, arXiv:1107.4616 [hep-ph].